

CREEP AND FATIGUE CRACK GROWTH IN PE-HD PIPE GRADES - EFFECT OF TEST TEMPERATURE AND R-RATIO

G. Pinter, W. Balika and R.W. Lang

Institute of Materials Science and Testing of Plastics
University of Leoben, A-8700 Leoben, Austria

ABSTRACT

The creep crack growth (CCG) and fatigue crack growth (FCG) behavior of two PE-HD pipe grades was studied based on a linear elastic fracture mechanics (LEFM) methodology. The FCG-tests were performed under a sinusoidal load at a frequency of 1 Hz and R-ratios (F_{\min}/F_{\max}) of 0.1, 0.3 and 0.5; the test temperatures were 23 (only FCG), 60 and 80 °C. The results showed that FCG rates in PE-HD are caused by a combination of cyclic-induced and creep-induced damage, depending on the mean stress level. While for given values of $K_{I\max}$ (FCG tests) and K_I (CCG tests), respectively, at low test temperatures the cyclic component of the applied stress dominates crack growth rates with CCG rates ($R = 1$) being lower than the FCG rates ($R < 1$), at high test temperatures the creep component becomes increasingly important in affecting crack growth rates so that CCG rates even exceed FCG rates. The point of inversion from fatigue to creep dominated failure on the temperature scale apparently depends on molecular and morphological characteristics of the PE-HD type and occurs at around 80 °C for PE-HD 1 and around 60 °C for PE-HD 2 in this investigation.

INTRODUCTION

Based on empirical findings of the failure behavior of pressurized plastics pipes in laboratory tests and on experiences with long-term field failures of pipes, linear elastic fracture mechanics (LEFM) concepts are frequently applied to also study the crack growth behavior of pipe grade poly(ethylenes) (PE). In the past the crack propagation behavior of various PE types was investigated using crack growth tests under static loads (so called creep crack growth (CCG) tests) [1-4]. More recently cyclic loading conditions (fatigue crack growth (FCG)) were used by some research groups to characterize the crack propagation resistance of PE [5-8].

However, while some studies on the failure behavior of notched specimens under static and fatigue loading conditions for a given PE type have been reported [9,10], so far hardly any information is available on a correlation between the kinetics of crack growth behavior under static and cyclic loads using LEFM concepts. Hence, it is the main objective of this paper to investigate the effects of R-ratio (minimum load to maximum load, F_{\min}/F_{\max} , in a fatigue cycle) on FCG behavior at various temperatures and to compare the results with the kinetics of crack growth under static loads. To gain some insight into the micromechanisms of crack growth under the various loading conditions, fracture surfaces were studied systematically via scanning electron microscopy (SEM).

GENERAL BACKGROUND

According to the concepts of linear elastic fracture mechanics (LEFM), the growth rate of a sharp crack in linear elastic materials with small scale plasticity is governed only by the applied stress intensity factor, K_I (index I stands for opening mode or pure tensile loading conditions), which describes the local crack tip stress and strain field [11]. The stress intensity factor, K_I , can in general be expressed as:

$$K_I = \sigma \cdot \sqrt{a} \cdot Y \quad (1)$$

where σ is the applied stress, a the crack length and Y is a non-dimensional correction function accounting for crack and component geometry as well as the type of loading.

Using these concepts CCG rates, da/dt , may then be plotted as a function of K_I and FCG rates, da/dN , may be controlled by the stress intensity factor range at the crack tip, $\Delta K_I = K_{I_{max}} - K_{I_{min}}$ [12]. Frequently, over a certain crack growth rate range an extended linear section is revealed on a double logarithmic scale by many plastics, indicating a power law relationship of the form

$$\frac{da}{dt} = A \cdot K_I^m \quad \text{for CCG} \quad (2)$$

$$\frac{da}{dN} = A' \cdot \Delta K_I^{m'} \quad \text{for FCG} \quad (3)$$

where A , A' and m , m' are constants, which depend on the material as well as on test variables such as temperature, environment, frequency and stress ratio. However, this relationship generally holds true only over an intermediate range of crack growth rates. When investigating a wide range of da/dt (da/dN), deviations from the power law may be observed as illustrated schematically in Fig. 1. That is, crack growth rates in region I, decrease rapidly to vanishingly small values as K_I (ΔK_I) approaches the threshold value, $K_{I_{th}}$ ($\Delta K_{I_{th}}$), and they increase markedly in region III as K_I ($K_{I_{max}}$) approaches the material's fracture toughness, K_{Ic} , and crack propagation becomes unstable.

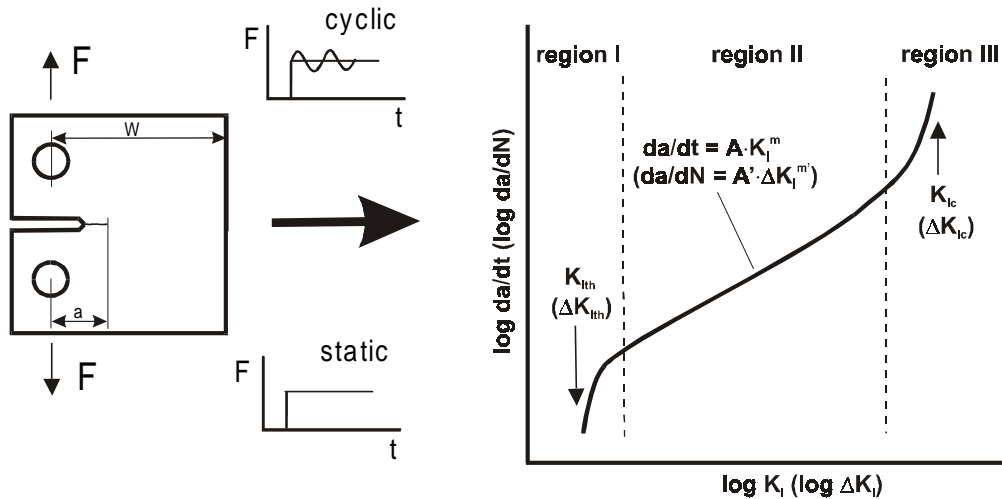


Figure 1: Schematic crack growth behavior of polymers under static and fatigue loads (F = force, W = specimen width, t = time)

EXPERIMENTAL

Two commercial grades of high density poly(ethylene) (PE-HD), produced by PCD Polymere Ges.m.b.H. (now Borealis AB, Linz, A) were used in this investigation. Relevant material properties for both material

types are listed in Table I.

For the CCG and FCG tests specimen of the compact type (C(T)) configuration (see Fig. 1) with a specimen width, W , of 40 mm were machined from 10 to 12 mm thick compression moulded plaques. All specimens were kept at a controlled temperature of 23 °C/50 % r.h. for at least 14 days before testing. Precracks were introduced into the test specimens prior to the fracture mechanical experiments by pressing a fresh commercial razor blade with a nominal thickness of 0.1 mm at room temperature into the V-notch tip.

TABLE I
MATERIAL CHARACTERIZATION AND MATERIAL PROPERTIES

Material-Code	ρ (23 °C/50 % r.h.) [g/cm ³]	X_C [%]	L_C [nm]	M_n [kg/mol]	M_w [kg/mol]	E (23 °C/50 % r.h.) [N/mm ²]	σ_Y (23 °C/50 % r.h.) [N/mm ²]
PE-HD 1	0.954	60	13	16	290	950	24
PE-HD 2	0.963	77	21	16	320	1400	30

(ρ = density; X_C = degree of crystallinity; L_C = lamella thickness; M_w = weight average molecular mass, M_n = number average molecular mass; E = elastic modulus; σ_Y = yield stress)

The CCG experiments were performed in a test apparatus, designed and constructed at the Institute of Materials Science and Testing of Plastics (University of Leoben, A). FCG testing was conducted with a servohydraulic closed-loop testing machine (MTS Systems GmbH, Berlin, D) under sinusoidal load control at a frequency of 1 Hz (to minimize hysteretic heating effects) and at R-ratios (F_{min}/F_{max}) of 0.1, 0.3 and 0.5. Both, CCG and FCG tests were performed in distilled water at 23, 60 and 80 °C, respectively, to simulate environmental conditions equivalent to hydrostatic stress rupture tests of pipes. Crack lengths values were monitored with the aid of travelling microscopes units equipped with linear variable transducers (LVTD) for displacement measurements.

Fractographic investigations of specific fracture surface details were carried out using a scanning electron microscope (SEM; Zeis, Oberkochen, D). Prior to the investigations all specimen were sputter coated with a 15 to 20 nm thick layer of gold. The operating voltage was 10 kV.

RESULTS AND DISCUSSION

Crack Growth Behavior

In order to verify the applicability of LEFM, constant ΔK_I and constant K_I experiments, respectively, were performed. Typical results are illustrated in Fig. 2 as da/dN and da/dt , respectively, versus the normalized crack length, a/W . The data depicted for both materials show remarkably constant crack growth rates with very little scatter over the entire a/W range, thus providing good support for the applicability of LEFM to these materials.

The FCG behavior of the two PE-HD types at different temperatures and an R-ratio of 0.1 is compared in Fig. 3. While PE-HD 1 exhibits superior FCG resistance over the entire temperature range, for both materials the FCG curves are shifted towards lower ΔK_I values with increasing test temperature. The improved behavior of PE-HD 1 is believed to be a result of the higher density of tie-molecules and the lower yield stress [13, 14].

FCG data for the three test temperatures illustrating the effects of variations in R-ratio at a given frequency are shown as a function of the applied stress intensity factor range, ΔK_I , in Fig. 4. Whereas the FCG resistance in terms of ΔK_I is markedly reduced for PE-HD 2 at all temperatures as the R-ratio is decreased, PE-HD 1 exhibits this effect only at 80 °C; at 60 °C the FCG curves for R = 0.1 and 0.3 and at 23 °C the curves for all R-ratios coincide.

Apparently mean stress effects on the fatigue response of PE-HD are controlled by conflicting processes. On the one hand there may be a tendency for higher crack growth rates at higher R-ratios as a result of more creep crack extension associated with the higher $K_{I\max}$ and mean stress intensity levels. Alternately, as the maximum plastic zone dimensions are expected to be controlled by $K_{I\max}$, higher R-ratios will lead to more extended plastic zone dimensions (craze dimensions), which act to blunt the crack and result in an increased tendency for strain energy dissipation, thus acting to reduce crack growth rates [12, 15, 16].

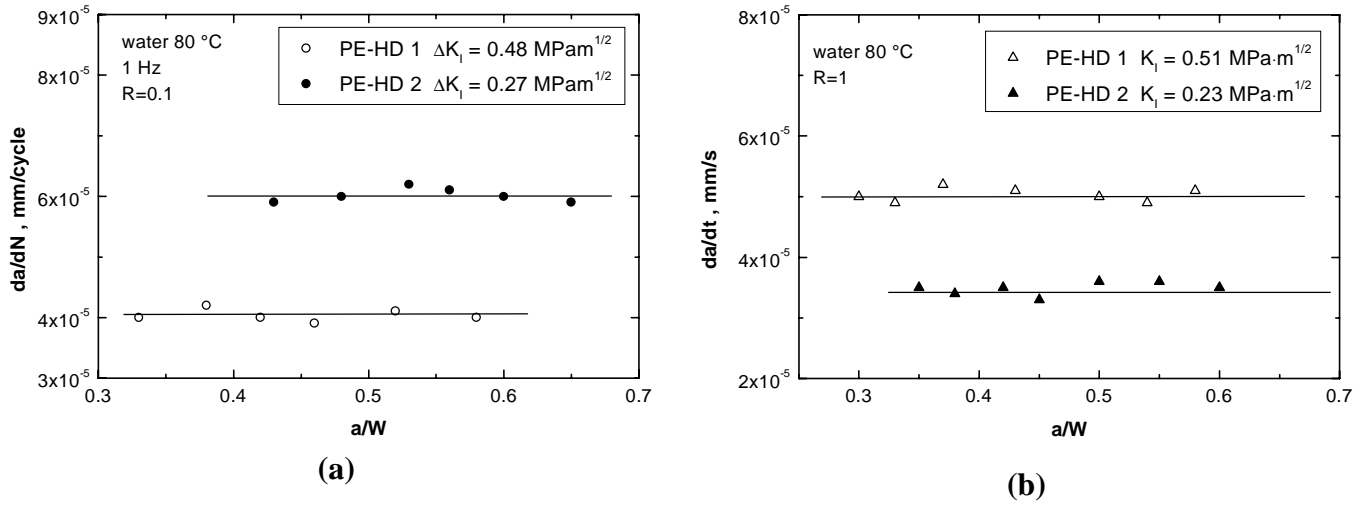


Figure 2: FCG rates (a) and CCG rates (b) in PE-HD under constant- ΔK_I and constant- K_I conditions, respectively

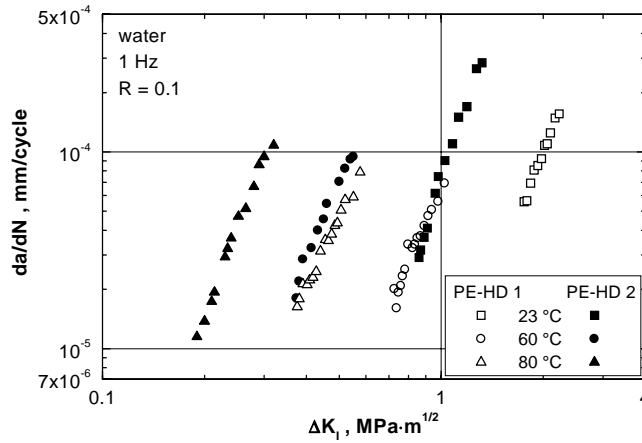


Figure 3: Influence of test temperature on FCG behavior in PE-HD

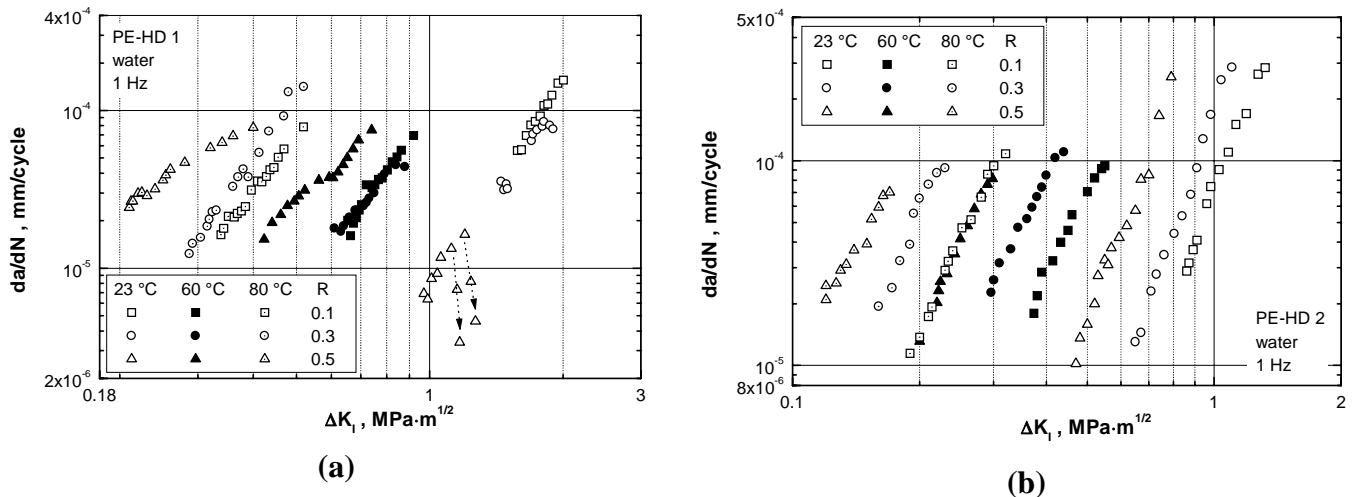


Figure 4: FCG rates of (a) PE-HD 1 and (b) PE-HD 2 for various R-ratios and temperatures as a function of ΔK_I

The just described phenomena are especially of relevance for PE-HD 1. At higher temperatures FCG rates are enhanced with higher R-ratios, whereas at lower temperatures larger plastic zones (crazes) with increasing R-ratio are responsible for relatively decreasing crack growth rates and even the arresting of cracks (i. e., in the case of $R = 0.5$, $23\text{ }^{\circ}\text{C}$). Such crack arrests could only be reinitiated by an increase in load. Another explanation for the coinciding curves at lower temperatures could be a decreasing influence of creep-induced damage.

In order to further investigate the effects of temperature on the significance of creep-induced and fatigue-induced damage, the FCG data of Fig. 4 are plotted in Fig. 5 in terms of $K_{I\max}$ together with data from CCG tests (the latter corresponding to the limiting case of a FCG test with an R-ratio of 1). In terms of $K_{I\max}$ both materials exhibit lower crack growth rates at higher R-ratios at $23\text{ }^{\circ}\text{C}$ due to the reduced ΔK_I -range. At higher temperatures, however, the differences between the crack propagation rates for various R-ratios vanish, so that at $60\text{ }^{\circ}\text{C}$ for PE-HD 2 and at $80\text{ }^{\circ}\text{C}$ for PE-HD 1 the curves for all R-ratios coincide. Apparently, at higher temperatures the decrease in da/dN at higher R-ratios (associated with the decrease in ΔK_I range) is almost balanced in PE-HD by an increase in da/dt (associated with the higher average K_I level), thus providing further evidence that creep-induced damage is more pronounced at higher temperatures.

In other words, while at low test temperatures the cyclic component of the applied stress dominates crack growth rates with CCG rates ($R = 1$) being lower than the FCG rates ($R < 1$), at high test temperatures the creep component becomes increasingly important in affecting crack growth rates so that CCG rates even exceed FCG rates at given values of $K_{I\max}$. The point of inversion from fatigue to creep dominated failure on the temperature scale apparently depends on molecular and morphological characteristics of a given PE-HD type and occurs at around $80\text{ }^{\circ}\text{C}$ for PE-HD 1 and around $60\text{ }^{\circ}\text{C}$ for PE-HD 2.

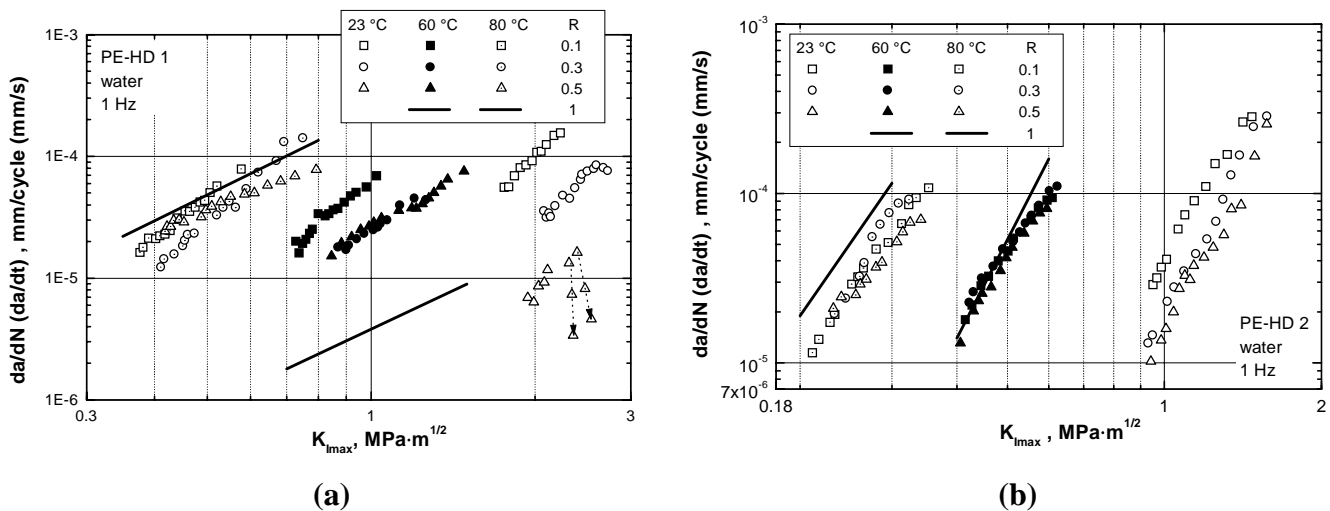


Figure 5: FCG rates of (a) PE-HD 1 and (b) PE-HD 2 for various R-ratios and temperatures as a function of $K_{I\max}$ and comparison with CCG data ($R = 1$)

Fracture Surface Morphology

Generally the fracture surfaces of both materials reveal the remnants of voids and fibrils, the typical attributes of craze formation and breakdown (see Fig. 6). Comparing the fracture surfaces of the two PE-HD types at equivalent ΔK_I values (Fig. 6a,b), it becomes apparent that the fibrils of PE-HD 2 are considerably less drawn than those of PE-HD 1, which on the one hand reflects the differences in the yield stress values of these materials and their effects on crack tip craze development. On the other hand, the higher tie molecule and interlamellar entanglement density of PE-HD 1 acts to stabilize the craze fibrils in the craze extension process prior to craze breakdown, leaving a more tufted structure with remnants of more highly stretched fibrils on the fracture surface. The higher tie molecule and interlamellar entanglement density of PE-HD 1 is of course also the prime reason for the superior CCG and FCG resistance of this PE-HD type [13, 14].

In Fig. 7 fracture surface details of PE-HD 2 tested at $60\text{ }^{\circ}\text{C}$ under cyclic loads with different R-ratios and with $K_{I\max}$ of $0.45\text{ MPa}\cdot\text{m}^{1/2}$, and under static load with a K_I value also of $0.45\text{ MPa}\cdot\text{m}^{1/2}$ are compared. For

all of these test conditions nearly equivalent crack growth rates of approximately $3 \cdot 10^{-5}$ mm/cycle (mm/s) were determined.

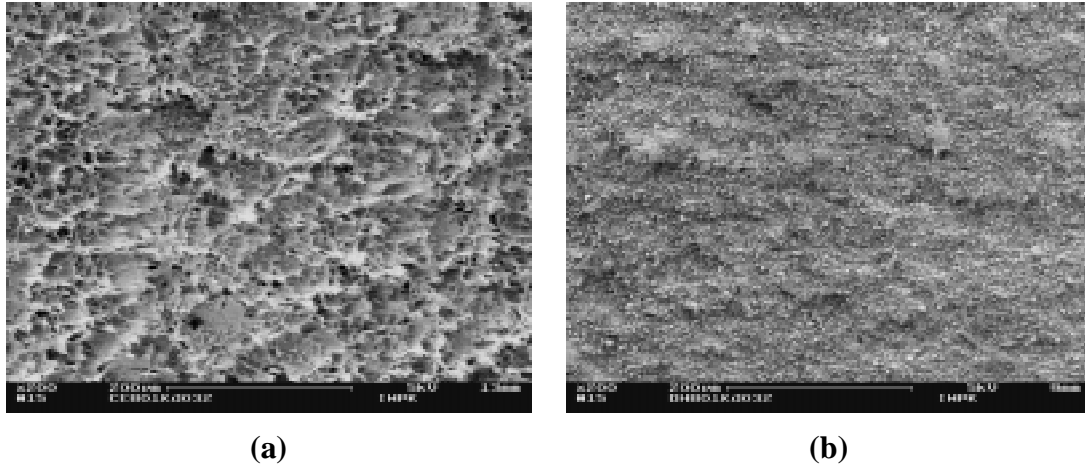


Figure 6: Comparison of the fracture surface of PE-HD 1 (a) and PE-HD 2 (b) at 80 °C and $\Delta K_I = 0.32$ $\text{MPa}\cdot\text{m}^{1/2}$

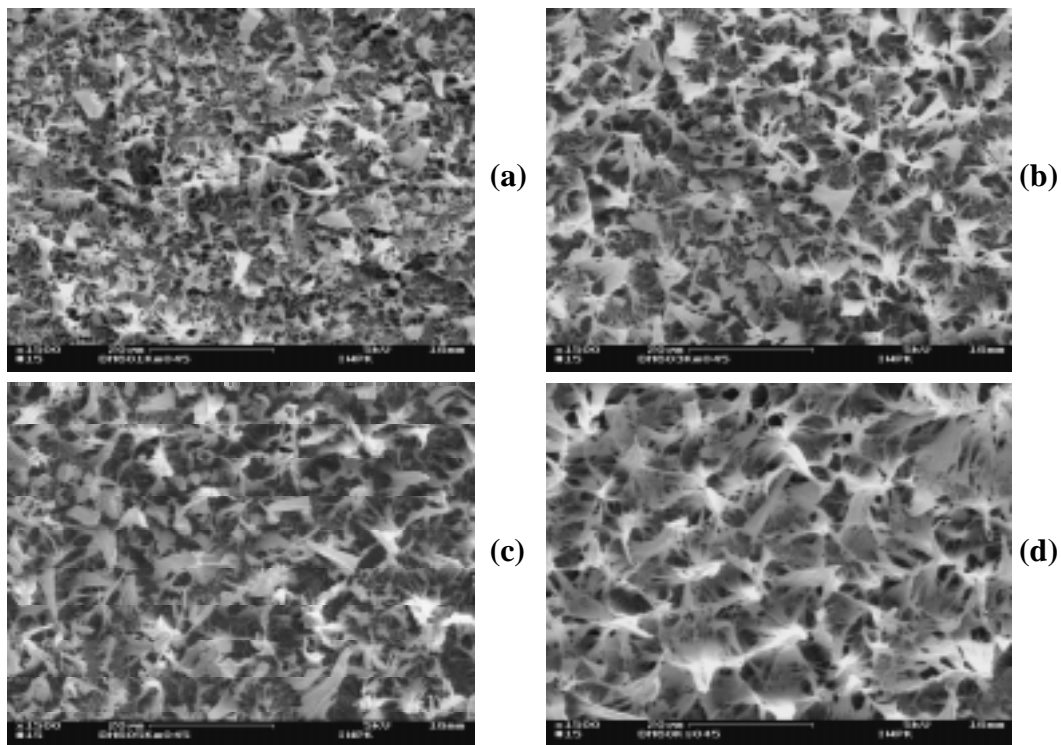


Figure 7: Comparison of the fracture surface of PE-HD 2 at 60 °C, constant $K_{I,\text{max}}$ resp. K_I values of 0.45 $\text{MPa}\cdot\text{m}^{1/2}$ and equal crack growth rates; (a) fatigue: $R = 0.1$, (b) fatigue: $R = 0.3$, (c) fatigue: $R = 0.5$, (d) static ($R = 1$)

Of special relevance to the observations in Fig. 7 it has been pointed out previously [16] that some influence of R-ratio at constant $K_{I,\text{max}}$ values on crack tip craze dimensions may be anticipated for viscoelastic materials, since a change in R-ratio also implies a change in the loading history. From the load-time traces illustrated in Fig. 8 it is evident that the loading rate (dF/dt and hence dK/dt) and the load-time integrated area per cycle at a constant value of the maximum load decrease and increase, respectively, as the value of R increases. Both of these factors will have some tendency to increase the crack-tip craze dimensions and the fibril extension with increasing R-ratio by decreasing the craze stress as a result of the smaller local strain rate, and by promoting creep and stress relaxation locally at the crack tip due to the higher average load.

Indeed, significant differences in crack tip craze zone dimensions were observed during the crack growth experiments, with larger crack tip craze zones being generated at given $K_{I,\text{max}}$ values with increasing R-ratio.

Hence, the pronounced influence of R-ratio (CCG tests corresponding to $R = 1$) on the micromorphology of fracture surfaces of PE-HD 2 in Fig. 7, with more highly stretched fibrils as the R-ratio is increased, apparently reflects the corresponding increase in craze zone dimensions.

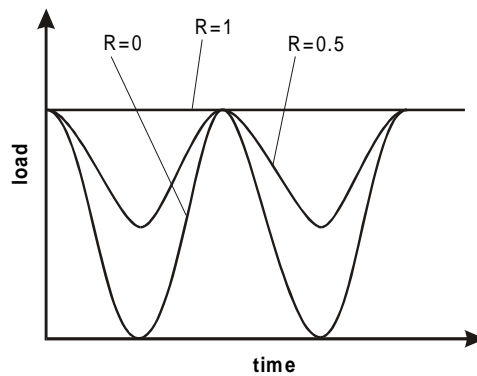


Figure 8: Comparison of two cyclic loads with a sinusoidal waveform at a constant maximum load but with different load-ratio, R

CONCLUSIONS

Based on FCG experiments with two types of PE-HD at various R-ratios from 0.1 to 0.5 and on CCG experiments (corresponding to an R-ratio of 1) in the temperature range from 23 to 80 °C, it could be shown that FCG rates in PE-HD are caused by a combination of cyclic-induced and creep-induced damage, depending on the mean stress level. While for given values of $K_{I\max}$ (FCG tests) and K_I (CCG tests), respectively, at low test temperatures the cyclic component of the applied stress dominates crack growth rates with CCG rates ($R = 1$) being lower than the FCG rates ($R < 1$), at high test temperatures the creep component becomes increasingly important in affecting crack growth rates so that CCG rates even exceed FCG rates. The point of inversion from fatigue to creep dominated failure on the temperature scale apparently depends on molecular and morphological characteristics of a given PE-HD type and occurs at around 80 °C for PE-HD 1 and around 60 °C for PE-HD 2.

The differences in the crack growth behavior of the two materials were interpreted in terms of molecular and morphological structure (i.e., interlamellar tie molecule and entanglement density, effects of the degree of crystallinity on yield stress) and on the resulting crack tip craze formation and breakdown processes. The mechanisms inferred were corroborated by fracture surface observations.

REFERENCES

- [1] Lustiger, A. and Markham, R.L. (1983) *Polymer*, **24**, 1647.
- [2] Egan, B.J. and Delatycki, O. (1995) *J. Mater. Sci.*, **39**, 3351.
- [3] Brown, N. and Lu, X. (1995) *Polymer*, **36**, 543.
- [4] Brown, N., Lu, X., Huang, Y.L., Harrison, I.P. and Ishikawa, N. (1992) *Plastics a. Rubber a. Composites Proces. a. Appl.*, **17**, 255.
- [5] Bucknall, C.B. and Dumpleton, P. (1995) *Plastics a. Rubber Proces. a. Appl.* **5**, 343.
- [6] Yeh, J.T. and Runt, J. (1991) *J. Polym. Sci.: Part B: Polym. Phys.* **29**, 371.
- [7] Strebel, J.J. and Moet, A. (1991) *J. Mat. Sci.* **26**, 5671.
- [8] Strebel, J.J. and Moet, A. (1995) *J. Polym. Sci.: Part B: Polym. Phys.* **33**, 1969.
- [9] Young, P., Kyu, T., Suehiro, S., Lin, J.S. and Stein, R.S. (1983) *J. Polym. Sci. Polym. Phys. Ed.* **21**, 881.
- [10] Reynolds, P.T. and Lawrence, C.C. (1991) *J. Mater. Sci.* **26**, 6197.
- [11] Kinloch, A.J. and Young, R.J. (1983). *Fracture Behaviour of Polymers*, Applied Science Publishers Ltd., Barking.

- [12] Hertzberg, R.W. and Manson, J.A. (1980). *Fatigue of Engineering Polymers*. Academic Press, New York.
- [13] Pinter, G. (1999). Dissertation, University of Leoben, Austria.
- [14] Pinter, G. and Lang, R.W. (2000) *Polymer*, in preparation.
- [15] Clark, T.R., Hertzberg, R.W. and Manson, A. (1990) *J. Testing a. Evaluation* **18**, 319.
- [16] Lang, R.W. (1984). Dissertation, Lehigh University, USA.